XXI IMEKO World Congress "Measurement in Research and Industry"
August 30 – September 4, 2015, Prague, Czech Republic

A BAYESIAN ANALYSIS TO EVALUATE THE NEUTRON RESPONSE OF A LIQUID SCINTILLATION SPECTROMETER

Marcel Reginatto [1], *Andreas Zimbal* [2]

[1] Physikalisch-Technische Bundesanstalt, Braunschweig, Germany, marcel.reginatto@ptb.de
[2] Physikalisch-Technische Bundesanstalt, Braunschweig, Germany, andreas.zimbal@ptb.de

Abstract – Many problems in neutron metrology require the determination of spectral neutron fluence rates. One of the prerequisites for doing spectrometry is the knowledge of the detector's response function. We report on a method to determine the response function of liquid scintillation spectrometers given measurements in monoenergetic neutron fields. The response function is modelled using radial basis functions and the parameters of the model are chosen using Bayesian parameter estimation.

Keywords: neutron metrology, neutron spectrometry

1. INTRODUCTION

Neutron spectrometry plays an important role in neutron metrology [1]. Detectors and dosemeters must be calibrated in known reference neutron fields and the characterization of these fields requires spectrometric measurements. These types of measurement are also needed for neutron dosimetry because the fluence-to-dose conversion factors for neutrons depend strongly on the energy of the incoming neutrons.

Detectors based on organic liquids scintillators (known under the names NE213 and BC501A) are routinely used for high resolution neutron spectrometry [2,3]. In scintillation detectors, the incoming neutrons interact with atomic nuclei and produce charged particles (mostly recoil protons but also alpha particles) and these charged particles in turn produce scintillation light. This light is collected in the detector to produce a pulse height spectrum (PHS), which is the outcome of the measurement. The PHS depends on the kinetic energy of the incoming neutrons. Thus, the analysis of the PHS will provide information on the neutron energy spectrum $\phi(E_n)$. An example of a PHS is given in Fig. 1, which shows a measurement of 8 MeV monoenergetic neutrons.

Neutron spectrometers are characterized by their response function, which describes the average number of counts to be expected in each of the channels of the PHS per incident neutron of a given energy E_n. To facilitate the comparison of measurements made under different experimental conditions, the x-axis of the PHS is usually labelled in terms of the light output L (which has units of energy) instead of channel number. Thus the response function $R(E_n,L)$ is a function of two continuous variables, E_n and L, and it may be visualized as a two-dimensional surface.

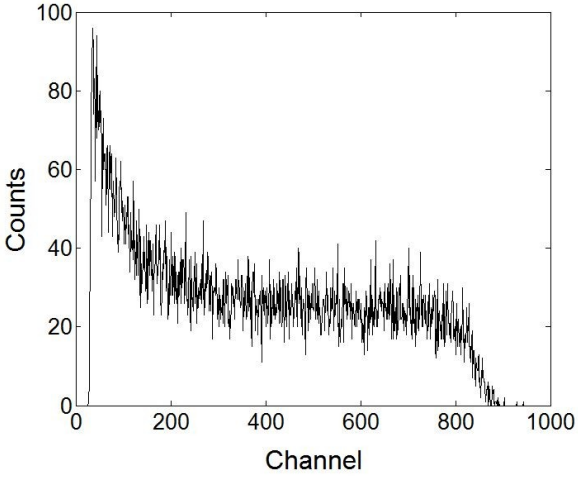

Fig. 1. Pulse height spectrum of a measurement of 8 MeV monoenergetic neutrons.

For computational reasons, it is convenient to introduce the response matrix R_{jk}, which is a discretization of the response function $R(E_n,L)$. The PHS measured by the spectrometer is related to the discretized neutron energy spectrum ϕ_k by the linear equations

$$N_j + \varepsilon_j = \sum_j R_{jk}\phi_k \qquad (1)$$

where N_j is the number of counts in channel j of the PHS, k labels the neutron energy, and ε_j is a term which accounts for effects such as statistical fluctuations in the number of counts, discrepancies which arise due to deviations of R_{jk} from the true value of the response matrix, experimental uncertainties, etc.

The goal of a spectrometric measurement is to derive the spectrum ϕ_k by solving Eq. (1) using deconvolution methods [4,5]. One of the prerequisites for doing spectrometry is the knowledge of the detector's response matrix. Thus, the response matrix plays a fundamental role in the analysis of the measurements. To carry out the deconvolution procedure successfully, it is necessary to have a response matrix that is as realistic as possible.

In this paper we propose a Bayesian method which allows us to determine the response function of liquid scintillation spectrometers given a set of measurements in

monoenergetic neutron fields, independent of numerical simulations of the response. We describe the method in detail and present results obtained for an analysis that covers the range of neutron energies 12 MeV < E_n <16 MeV of the response matrix. The application of the approach to the full response matrix is in principle straightforward but computationally demanding, thus it will be addressed in a forthcoming publication. Here we focus on the method and on conceptual issues.

The paper is organized as follows. In the next section we discuss two approaches for the determination of neutron response matrices for NE213 liquid scintillators, one based on numerical simulations and the other one based on measurements. The following section is devoted to a description of the Bayesian approach that we propose for the analysis of a set of measurements of the spectrometer's response. After that we present results of the analysis. We end the paper with a summary.

2. DETERMINATION OF THE NEUTRON RESPONSE MATRIX

The standard way of determining the neutron response matrix of a liquid scintillation spectrometer [2,6] is to combine measurements in monoenergetic neutron reference fields with numerical simulations of the response function. Fig. 2 shows a contour plot of a response matrix calculated using this standard procedure. The plot uses a logarithmic scale (base 10) to display the response because it has a range that extends over a few orders of magnitude.

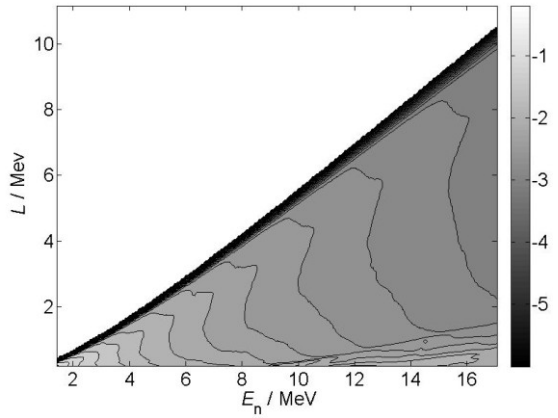

Fig. 2. Contour plot of the common logarithm of the response, for a response matrix based on numerical simulations.

When following this approach, we have used the Monte Carlo code NRESP [7] which can simulate PHS for a given detector cell geometry and neutron energy. However, the simulated response calculated by NRESP has features which are sharper than the ones observed in actual measurements; therefore, it is necessary to adjust the simulated response matrix to fit calibration measurements. This adjustment process is a non-trivial procedure which involves a number of elaborate steps, including an energy dependent Gaussian broadening of the simulated response matrix [2,6,8]. Although the standard approach has proven to be very powerful, there are certain limitations to it. Furthermore, it is not possible to simulate exactly all the nuclear reactions that need to be included in the calculation of the response matrix, and this leads to minor but observable discrepancies between simulations and measurements.

A better alternative, when possible, is to determine these response functions solely from experiment [8,9,10]. This can be done; however, the measurements of the response typically contain a fair amount of statistical fluctuations (see for example the measurement shown in Fig. 1). In principle, the statistics of the measurements can be reduced by using longer measurement times. In practice, this is not feasible. Therefore, it becomes necessary to use data analysis procedures to address this issue. This requires some care because a simple smoothing procedure will change the shape of the response function, and this in turn will affect the neutron energy spectrum that is obtained when a deconvolution of the data is carried out (in particular, the widths of peaks will be affected). Thus, for applications in metrology, a more careful approach is required. It is for this reason that we propose the method that we describe in the next section.

3. BAYESIAN ANALYSIS OF MEASUREMENTS OF THE DETECTOR RESPONSE

Measurements of the detector response [8,9,10] result in a matrix D_{jk} which may be visualized as a two-dimensional surface. This matrix is related to the spectrometer's response R_{jk} by an equation of the form

$$D_{jk} = R_{jk} + \varepsilon_{jk} \tag{2}$$

where the discrepancy between D_{jk} and R_{jk} (i.e., the term ε_{jk}) is due primarily to counting statistics.

Due to the physics of scintillation spectrometers, the response is expected to be smooth, without sharp peaks or shoulders. Thus, to model R_{jk}, we may introduce thin plate splines, which are a particular type of radial basis functions. Using the notation $x = E_n, y = L$, the model of the response function is written in the form [11]

$$R_{jk} = \sum_{i=1}^{n} \lambda_i \phi_{ijk} + \mu_1 + \mu_2 x_j + \mu_3 y_k, \tag{3}$$

where n is the number of centres, (x_i, y_i) is the location of the centres, $r_{ijk}^2 = (x_i - x_j)^2 + (y_i - y_k)^2$, the radial basis function $\phi_{ijk} = r_{ijk}^2 \ln(r_{ijk})$, and λ_i and μ_l are parameters which have to be determined by fitting the response R_{jk} to the measurements D_{jk}.

To determine these unknown parameters, we use Bayesian parameter estimation [12]. We now discuss the main features of the approach.

3.1. Likelihood function and priors

The data D_{jk} used for the analysis consist of a large number of PHS from measurements of monoenergetic neutrons. The uncertainty in the data is mainly due to counting statistics, with typically enough counts in each channel for the normal approximation to be valid. Therefore, it is appropriate to choose a likelihood function of the form

$$P(D_{jk}|\lambda_i,\mu_l) \sim exp\left\{-\frac{1}{2}\sum_{j,k}\frac{[D_{jk}-R_{jk}(\lambda_i,\mu_l)]^2}{\sigma_{jk}^2}\right\}, \qquad (4)$$

where the standard deviations σ_{jk} are set equal to the square root of the number of counts in the corresponding channel.

The model depends on the parameters λ_i and μ_l. We chose reference priors for these parameters (i.e., uniform distributions) since in our case informative priors are neither justified nor necessary.

3.2. Choice of centers

To enforce smoothness of R_{jk}, it is desirable to minimize the number of centres used for the model. However, the number of centres has to be sufficient to provide a good fit to the measurements D_{jk}. These two competing requirements may be satisfied by choosing an optimal number of centres distributed according to the amount of structure that is present in the response function, in the following way.

It will be convenient to visualize the response function as a two-dimensional surface. Then, intuitively, one would like to have a higher density of centers in those areas in which the curvature of the surface is high (i.e., areas with peaks and valleys) and a lower density of centers in those areas in which the curvature of the surface is low (i.e., areas that are flat or close to flat).

To make this intuitive idea more precise, we need to define in a more formal way what we mean by curvature. One way of doing this is to introduce the Gaussian curvature. Given a two-dimensional surface z(x,y), the Gaussian curvature K is defined by

$$K = \frac{(\partial^2 z/\partial x^2)(\partial^2 z/\partial y^2)-(\partial^2 z/\partial x\partial y)}{[1+(\partial z/\partial x)^2+(\partial z/\partial y)^2]^2}. \qquad (5)$$

Fig. 3 shows a plot of the magnitude of the Gaussian curvature for a response matrix obtained using the standard approach discussed in section 2 (i.e., a response matrix based on Monte Carlo simulations).

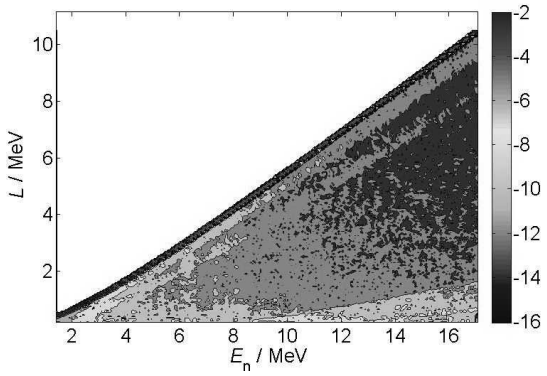

Fig. 3. Contour plot of the common logarithm of the magnitude of the Gaussian curvature, for a response matrix based on numerical simulations.

The plot uses a logarithmic scale because the absolute value of the curvature |K| has a range that extends over several orders of magnitude. The evaluation of the Gaussian curvature was carried out with a program written in Matlab [13], using built-in routines for the calculation of partial derivatives.

Another possibility is to calculate the curvature along fixed values of the neutron energy E_n, which is physically meaningful in this context because it corresponds to calculating the curvature of each of the PHS that make up the response matrix. This curvature is given by

$$C = \frac{\partial^2 z/\partial y^2}{[1+(\partial z/\partial y)^2]^{2/3}}. \qquad (6)$$

Fig. 4 shows the same plot as Fig. 3, but in this case replacing the magnitude of the Gaussian curvature K by the magnitude of C.

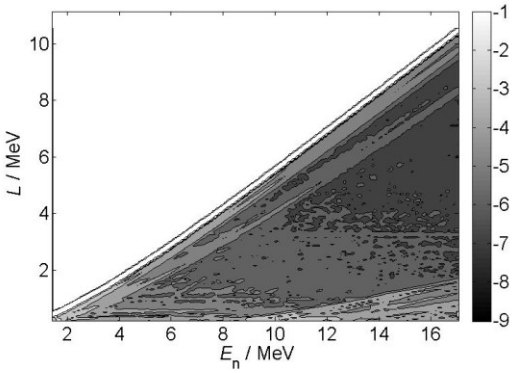

Fig. 4. Contour plot of the common logarithm of the magnitude of the curvature along PHS, for a response matrix based on numerical simulations.

Figs. 3 and 4 indicate that there are two regions where the curvature is highest: the area which is close to the lower boundary (i.e., close to the line L = 0.4 MeV), and the area which is close to the diagonal line which separates the region where the response is zero (above the diagonal) from the region where the response is positive (below the diagonal). The intermediate region has lower curvature. This suggests that the first two regions require a higher density of centers than the intermediate region.

While the curvature plots proved to be helpful for choosing the placement of the centers, we do not have at this time a simple algorithm that can make the procedure automatic. Therefore, the placement of the centers still requires a certain degree of trial and error. More details on the choice of centers will be given below in section 4 where we present results of the analysis.

3.3. Choice of optimal parameters

As described in section 3.1, we carry out the Bayesian analysis with the likelihood function of Eq. (4) and priors for the parameters λ_i and μ_l which are uniform. Under these

conditions, Bayes' theorem leads to a posterior probability which is proportional to the likelihood function.

Our best estimate of λ_i and μ_l is given by the choice of parameters that maximize the posterior; i.e., the values of λ_i and μ_l at the mode of the posterior probability. For computational reasons, it is convenient to search for the maximum of the logarithm of the posterior distribution [12], which in our case is given by

$$log\left[P\left(D_{jk}\middle|\lambda_i,\mu_l\right)\right] \sim -\frac{1}{2}\sum_{j,k}\frac{\left[D_{jk}-R_{jk}(\lambda_i,\mu_l)\right]^2}{\sigma_{jk}^2} \quad . \qquad (7)$$

The maximum of the mode can be calculated by finding the point in parameter space where the derivatives of the logarithm of the posterior distribution with respect to the λ_i and μ_l are zero. For Eq. (7), this procedure leads to a set of equations which is linear in the parameters [12]. Thus the equations that determine the optimal values of λ_i and μ_l can be solved using matrix inversion methods. We carried out this procedure with a program written in Matlab [13].

4. RESULTS

The data set available for the analysis is in the form of a matrix D_{jk} with j=1,...,2236 and k=1,...,1061. We are dealing therefore with a fairly large data set of ~10^6 measurements. The light output covers the range 0.4 MeV < L < 10.3 MeV and the neutron energy the range 1.4 MeV < E_n < 17.0 MeV.

To test the method described in section 3, we carried out an analysis on a subset of the data. The application of the approach to the full response matrix is in principle straightforward but computationally demanding, thus we restrict here to a subset of the data which extends over the range 0.4 MeV < L < 10 MeV of light output and the range 12 MeV < E_n < 16 MeV of neutron energies.

Based on the curvature plots (see Figs. 3 and 4), we defined the following three regions: Region 1, extending from L = 0.4 MeV to L = 2.2 MeV; Region 2, extending from L = 2.2 MeV to the diagonal line with the equation $L(E_n)$ = (0.74 E_n – 3.15); and Region 3, extending from the diagonal line with the equation $L(E_n)$ = (0.74 E_n - 3.15) to the diagonal line with the equation $L(E_n)$ = (0.74 E_n - 1.65).

In Region 1, we placed the centers along nine lines of constant E_n separated by intervals of 0.5 MeV, while in Regions 2 and 3 it was sufficient to place the centers along five lines of constant E_n separated by intervals of 1.0 MeV. In Regions 1, 2 and 3, we placed the centers at intervals of L = 0.25 MeV, L = 0.75 MeV, and L = 0.20 MeV, respectively. Thus Regions 1 and 3 have a higher density of centers than Region 2.

As mentioned previously, while the plots of curvature (Figs. 3 and 4) provide valuable insight, we do not have at this time a simple algorithm that can make the placement of the centers automatic. Therefore, this procedure still requires a certain degree of trial and error, and its ultimate justification is given by the quality of the results.

Figs. 5, 6 and 7 show results for three neutron energies, E_n = 12.25 MeV, E_n = 15.25 MeV, and E_n = 16 MeV. These particular values of E_n were chosen because they correspond to PHS located towards the boundaries of the interpolation region, where two-dimensional interpolation methods often encounter difficulties. Thus, they provide a good test of the method.

Fig. 5 corresponds to a measurement made with a value of E_n which is at the lower end of the neutron energy region of the fit (12 MeV < E_n <16 MeV). The fit to the data follows the measurement quite well and it does not display artefacts despite the fact that there are no centers located along this particular value of E_n.

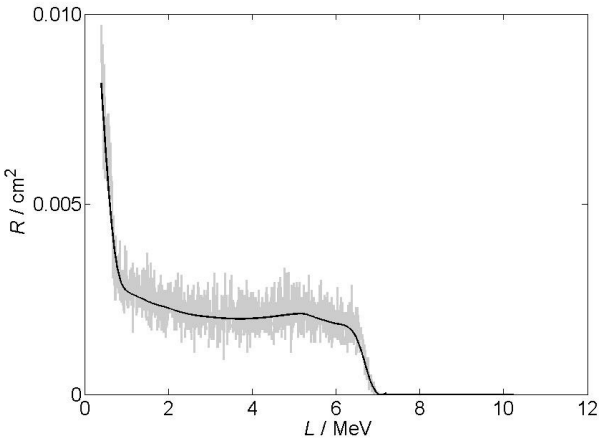

Fig. 5. Measurement (grey) and response derived using the Bayesian approach (black) for 12.25 MeV monoenergetic neutrons.

Fig. 6 corresponds to a measurement made with a value of E_n which is at the higher end of the neutron energy region of the fit (12 MeV < E_n <16 MeV). Once more, the fit to the data follows the measurement quite well and it does not display artefacts despite the fact that also in this case there are no centers located along this particular value of E_n.

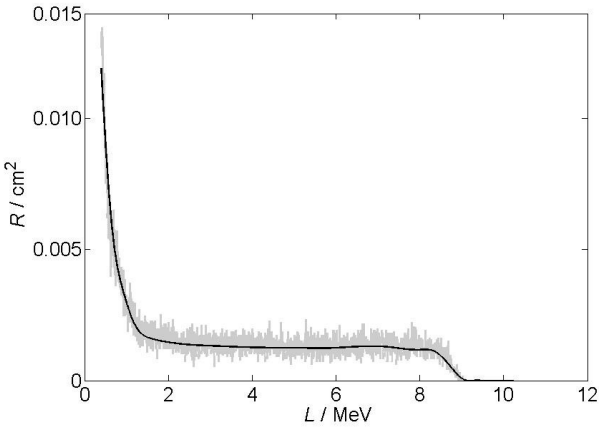

Fig. 6. Measurement (grey) and response derived using the Bayesian approach (black) for 15.25 MeV monoenergetic neutrons.

Finally, Fig. 7 corresponds to a measurement made with a value of E_n which is at the boundary of the neutron energy region of the fit (12 MeV < E_n <16 MeV). Notice that there is some structure below L = 2 MeV; this structure is due to nuclear reactions that result from the interaction of neutrons

of this energy with carbon nuclei. This structure, which does not appear in Fig. 6, is followed quite well by the fit.

In all three cases, the response derived from the Bayesian approach fits very well the measurements. This remains true of other similar examples.

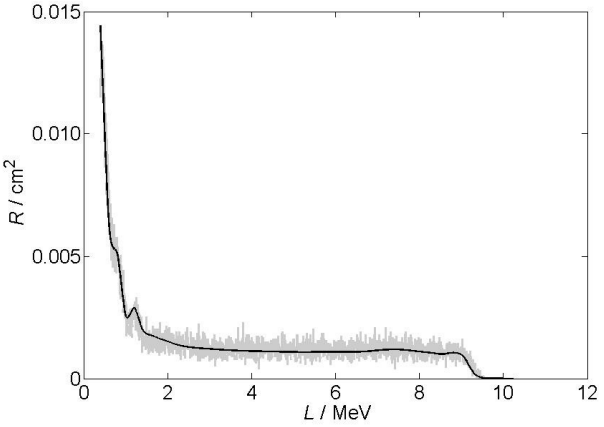

Fig. 7. Measurement (grey) and response derived using the Bayesian approach (black) for 16 MeV monoenergetic neutrons.

5. SUMMARY

We presented a Bayesian method which allows us to determine the neutron response matrix of liquid scintillation spectrometers given a set of measurements in monoenergetic neutron fields. The response matrix was modelled using thin plate splines, which are a particular type of radial basis functions. The parameters of the model were chosen using Bayesian parameter estimation methods. The method is to a large extent independent of numerical simulations of the response, which are only used to guide the choice of centers.

We discuss two issues which require further development. First, the choice of centers for the radial basis functions interpolation. We have proposed an approach that is guided by plots of the curvature of simulated response functions. While these plots have proven to be helpful, an algorithm based on the curvature that can automatically choose the centers is still not available. We intend to extend this work, with the aim of determining a general method that can accomplish this. Second, while the application of our approach to the full response matrix is in principle straightforward, in practice it is computationally demanding and for this reason we have presented results which are based on only a limited amount of data, covering only part of the full response matrix. The next step is to extend our method to the full response matrix.

REFERENCES

[1] D. J. Thomas, R. Nolte and V. Gressier, "What is neutron metrology and why is it needed?", *Metrologia* 48, S225–S238, 2011.

[2] H. Klein and S. Neumann, "Neutron and photon spectrometry with liquid scintillation detectors in mixed fields", *Nucl. Instrum. Meth. A* 476, 132-142, 2002.

[3] H. Klein, "Neutron spectrometry in mixed fields: NE213/BC501A liquid scintillation spectrometers", *Radiat. Prot. Dosimetry* 107, 95-109, 2003.

[4] M. Reginatto, "Overview of spectral unfolding techniques and uncertainty estimation", *Radiat. Meas.* 45, 1323-1329, 2010.

[5] M. Reginatto and A. Zimbal, "Bayesian and maximum entropy methods for fusion diagnostic measurements with compact neutron spectrometers", *Rev. Sci. Instrum.* 79, 023505, 2008.

[6] D. Schmidt, B. Asselineau, R. Böttger, H. Klein, L. Lebreton, S. Neumann, R. Nolte, G. Pichenot, "Characterization of liquid scintillation detectors", *Nucl. Instrum. Meth. A* 476, 186–189, 2002.

[7] G. Dietze and H. Klein, "NRESP4 and NEFF4: Monte Carlo Codes for the Calculation of Neutron Response Functions and Detection Efficiencies for NE213 Scintillation Detectors", PTB Report PTB-ND-22, 1982.

[8] F. Gagnon-Moisan, M. Reginatto and A. Zimbal, "Results for the response function determination of the Compact Neutron Spectrometer", *Proceedings of the 2nd International Workshop on Fast Neutron Detectors and Applications*, Ein Gedi, Israel, November 6-11, JINST 7, C03023, 2012.

[9] A. Hildebrand, H. Park, S. Khurana, R. Nolte, D. Schmidt, "Experimental Determination of the Response Matrix of a BC501A Scintillation Detector using a Wide Neutron Spectrum: A Status Report", Laboratory Report PTB-6.42-05-1, 2005.

[10] A. Zimbal, H. Klein, M. Reginatto, H. Schuhmacher, L. Bertalot, A. Murari, and the JET-EFDA Contributors, "High resolution neutron spectrometry with liquid scintillation detectors for fusion applications", *Proceedings of the 1st International Workshop on Fast Neutron Detectors and Applications*, Cape Town, South Africa, April 3–6, 2006, PoS(FNDA2006)035.

[11] S. K. Lodha and R. Franke, "Scattered data techniques for surfaces", *DAGSTUHL '97 Proceedings of the Conference on Scientific Visualization*, edited by H. Hagen, G. Nielson, and F. Post, IEEE Computer Society, Washington, DC, 1997.

[12] D. S. Sivia and J. Skilling, *Data Analysis – A Bayesian Tutorial*, 2nd edition, Oxford University Press, Oxford, 2006.

[13] MATLAB and Statistics Toolbox Release 2010a, The MathWorks, Inc., Natick, Massachusetts, United States.